

Analog of astrophysical magnetorotational instability in a Couette-Taylor flow of polymer fluids

Stanislav Boldyrev, Don Huynh, and Vladimir Pariev*

Department of Physics, University of Wisconsin—Madison, 1150 University Avenue, Madison, Wisconsin 53706, USA

(Received 24 June 2008; revised manuscript received 12 June 2009; published 15 December 2009)

We report experimental observation of an instability in a Couette-Taylor flow of a polymer fluid in a thin gap between two coaxially rotating cylinders in a regime where their angular velocity decreases with the radius while the specific angular momentum increases with the radius. In the considered regime, neither the inertial Rayleigh instability nor the purely elastic instability is possible. We propose that the observed “elastorotational” instability is an analog of the magnetorotational instability which plays a fundamental role in astrophysical Keplerian accretion disks.

DOI: [10.1103/PhysRevE.80.066310](https://doi.org/10.1103/PhysRevE.80.066310)

PACS number(s): 47.57.Ng, 52.30.Cv, 95.30.Qd

I. INTRODUCTION

Accretion is a fundamental process in astrophysics by which protostellar objects and stars are formed. Due to gravity, the interstellar gas collapses into thin disks differentially rotating around accreting bodies. As angular momentum is conserved, in order for the gas to further fall onto the central object, angular momentum has to be transported out of the system. Since the molecular viscosity in disks is very small, the laminar Keplerian disk cannot lose its angular momentum by frictional forces on astrophysically reasonable time scales. The need for much larger, possibly turbulent angular momentum transport was identified in Lynden-Bell [1] and Shakura and Syun'yaev [2], although it remained unclear what could make a hydrodynamically stable Keplerian flow turbulent. In the 1990s, it was realized that a weak magnetic field existing in accretion disks leads to a quickly growing instability rendering the disks turbulent. This is the magnetorotational instability (MRI) originally derived by Velikhov [3] and Chandrasekhar [4] and rediscovered in astrophysical context by Balbus and Hawley [5].

During the last decade, considerable progress has been made in understanding the effects of such instability on differentially rotating flows. A sizable amount of analytic work was devoted to linear analysis of instability thresholds (e.g., [6–8]). Extensive numerical simulations of the nonlinear stage of the magnetorotational instability have also been performed, e.g., [9–13], however, it still remains a challenge to address the ranges of scales relevant for real astrophysical systems. Laboratory investigations of the magnetorotational instability in liquid-metal experiments have been proposed (e.g., [14–18]) and conducted [19,20]. However, large resistivity of liquid metals complicates unambiguous laboratory study of the magnetorotational instability. Recently, however, the instability was observed in a Couette-Taylor liquid-metal experiment where the helical rather than “standard” axial magnetic field was applied by external coils [21]. The relevance of this setting for Keplerian accretion disks is discussed in [22].

In the present paper, we report a laboratory observation of an analog of astrophysical magnetorotational instability in an

experiment using viscoelastic solutions of high molecular weight polymers. In a certain range of parameters, the dynamic equations describing viscoelastic polymer fluids are identical to the magnetohydrodynamic equations describing conducting fluids or plasmas. This opens a way to investigate the fundamental astrophysical instability in a simple laboratory setting.

To explain the physics of the instability, consider two fluid elements rotating at different orbits and connected by an elastic string (a magnetic field in accretion disks, a polymer in our experiment). The inner element rotates faster, therefore, it is pulled back by the string. As a result, it loses its angular momentum and falls closer to the center. The outer fluid element is pulled forward, gains angular momentum, and goes to a larger orbit. The fluid elements thus move apart stretching the string even more, leading to the instability.

Our interest to the problem was motivated by analytic work of Ogilvie and Proctor [23] elucidating the analogy between instabilities in Couette-Taylor flows of magnetic and polymer fluids. (When our experiment was in progress, we became aware of the new paper by Ogilvie and Potter [24], where this analogy is developed in more detail.) The experiment provides an intriguing possibility to investigate the regime of “elastorotational” instability and resulting elastorotational turbulence in non-Newtonian polymer fluids; such regimes have not been experimentally studied before. From a practical point of view, polymer solutions are relatively inexpensive and nonhazardous. The experiment is suitable for undergraduate projects and lecture demonstration.

A. Magnetohydrodynamics and polymer fluid dynamics

The dynamics of a conducting fluid is described by the set of magnetohydrodynamic (MHD) equations

$$\partial_t \mathbf{v} + (\mathbf{v} \cdot \nabla) \mathbf{v} = -\nabla p + (\mathbf{B} \cdot \nabla) \mathbf{B} + \eta \Delta \mathbf{v} + \mathbf{F}, \quad (1)$$

$$\partial_t \mathbf{B} + (\mathbf{v} \cdot \nabla) \mathbf{B} - (\mathbf{B} \cdot \nabla) \mathbf{v} = \eta_M \Delta \mathbf{B}, \quad (2)$$

where $\mathbf{v}(\mathbf{x}, t)$ is the velocity field, $\mathbf{B}(\mathbf{x}, t)$ is the magnetic field normalized by $\sqrt{4\pi\rho}$, p is pressure, which includes the magnetic part, η is fluid viscosity, and η_M resistivity. We assume that the fluid is incompressible and the density is constant, say $\rho=1$. The external force $\mathbf{F}(\mathbf{x}, t)$ represents mechanisms

*Present address: Korea Astronomy and Space Science Institute, 61-1, Hwaam-dong, Yuseong-gu, Daejeon 305-348, South Korea.

driving the flow. We also assume cylindrical geometry with the coordinates r , θ , and z , where the steady state is described by the azimuthal velocity field $v_\theta(r)$. For the gravitational force, $F_r \propto -1/r^2$, the velocity field has the Keplerian profile $v_\theta(r) \propto r^{-1/2}$.

As follows from Eq. (1), the back reaction of the magnetic field on the flow is described by the Maxwell electromagnetic stress tensor $T_M^{ij} = B^i B^j$. The evolution equation for this tensor is derived from Eq. (2), where we neglect small resistivity η_M

$$\partial_t T_M^{ij} + (\mathbf{v} \cdot \nabla) T_M^{ij} - T_M^{ij} \nabla_i v^j - T_M^{il} \nabla_l v^j = 0. \quad (3)$$

The tensor $T_M^{ij} = B^i B^j$ obeying this equation is said to be “frozen” into the flow. In the case of polymer fluids, the polymer stress tensor T_p^{ij} frozen into the flow should obey the same equation.

In contrast with a magnetic fluid, there is no exact equation describing the dynamics of polymer solutions. However, in the case when a solution is dilute, one can formulate the constitutive equations based on general principles of fluid dynamics [25,26]. The stress tensor can be represented as a linear sum of the viscous stress of the solvent $T^ij = \eta(\nabla_i v^j + \nabla_j v^i)$ and the stress T_p^{ij} contributed by the polymer. The polymer contribution should generally obey the equation

$$T_p^{ij} + \tau D_t T_p^{ij} = \eta_p (\nabla_i v^j + \nabla_j v^i). \quad (4)$$

Here, τ is the relaxation time of the fluid element, which is related to polymer elasticity, and D_t denotes the convective derivative, as in Eq. (3),

$$D_t T_p^{ij} \equiv \partial_t T_p^{ij} + (\mathbf{v} \cdot \nabla) T_p^{ij} - T_p^{ij} \nabla_i v^j - T_p^{il} \nabla_l v^j. \quad (5)$$

If the relaxation time τ is very large compared to a characteristic time of the flow, the second term on the left hand side of Eq. (4) dominates, and the stress is advected by the fluid. In the other limit, $\tau \rightarrow 0$, the polymer is not frozen into the fluid—it rapidly relaxes to its nonstretched equilibrium configuration and contributes to fluid viscosity, $T_p^{ij} = \eta_p (\nabla_i v^j + \nabla_j v^i)$. The dynamics of the velocity field in Eq. (5) is given by the standard Navier-Stokes equation of motion

$$\partial_t \mathbf{v} + (\mathbf{v} \cdot \nabla) \mathbf{v} = -\nabla p + \nabla \cdot \mathbf{T}_p + \eta \Delta \mathbf{v} + \mathbf{F}. \quad (6)$$

The systems (4)–(6) present the so-called B model of Oldroyd [26], a constitutive system for dilute polymer solutions.

B. Ogilvie-Proctor model

The analogy of MHD and polymer fluid instabilities in the Couette-Taylor regime was elucidated by Ogilvie and Proctor [23]. Following their work, we change the variable: $T_p^{ij} \rightarrow \tilde{T}_p^{ij} = T_p^{ij} + \frac{\eta_p}{\tau} \delta^{ij}$, where δ^{ij} is the Kronecker delta. The momenta Eqs. (1) and (6) for magnetic and polymer fluids now have identical forms

$$\partial_t \mathbf{v} + (\mathbf{v} \cdot \nabla) \mathbf{v} = -\nabla p_M + \nabla \cdot \mathbf{T}_M + \eta \Delta \mathbf{v} + \mathbf{F}, \quad (7)$$

$$\partial_t \mathbf{v} + (\mathbf{v} \cdot \nabla) \mathbf{v} = -\nabla p_p + \nabla \cdot \tilde{\mathbf{T}}_p + \eta \Delta \mathbf{v} + \mathbf{F}, \quad (8)$$

where the pressure terms ensure incompressibility of the flows. The dynamic equations for the stress tensors are

$$\begin{aligned} \partial_t T_M^{ij} + (\mathbf{v} \cdot \nabla) T_M^{ij} - T_M^{ij} \nabla_i v^j - T_M^{il} \nabla_l v^j \\ = \eta_M [B^i \nabla^2 B^j + (\nabla^2 B^i) B^j], \end{aligned} \quad (9)$$

$$\begin{aligned} \partial_t \tilde{T}_p^{ij} + (\mathbf{v} \cdot \nabla) \tilde{T}_p^{ij} - \tilde{T}_p^{ij} \nabla_i v^j - \tilde{T}_p^{il} \nabla_l v^j = -\frac{1}{\tau} \left[\tilde{T}_p^{ij} - \frac{\eta_p}{\tau} \delta^{ij} \right]. \end{aligned} \quad (10)$$

These equations are identical except for the dissipation terms—the magnetic field diffuses while the polymer stress relaxes. However, if the magnetic Reynolds number $\text{Rm} \sim \Omega d^2 / \eta_M$ and the Weissenberg number $\text{Wi} = \tau |\partial \Omega / \partial (\ln r)| \sim \tau \Omega$ are large (Ω being the angular velocity and d the gap between cylinders), one can neglect the dissipation terms.

Denote R_1 and R_2 as the inner and outer radii, respectively. When the gap is narrow, $d/R \ll 1$, the shearing rate of the basic flow, which is a Couette-Taylor flow, may be assumed to be constant in the gap, $\dot{\gamma} \equiv \partial v_\theta / \partial r - v_\theta / r = r \partial \Omega / \partial r \approx \text{const}$. The corresponding stationary solution of Eq. (10) in coordinates (r, θ, z) then has the form [23]

$$\tilde{\mathbf{T}}_p = \frac{\eta_p}{\tau} \begin{bmatrix} 1 & -\text{Wi} & 0 \\ -\text{Wi} & 2\text{Wi}^2 + 1 & 0 \\ 0 & 0 & 1 \end{bmatrix}. \quad (11)$$

There is no exact correspondence of the tensor (11) to the magnetic tensor \mathbf{T}_M , since Eq. (11) cannot be represented as a product of two vector fields. However, one can introduce a set of three auxiliary fields, \mathbf{B}_1 , \mathbf{B}_2 , and \mathbf{B}_3 , such that

$$\tilde{T}_p^{ij} = B_1^i B_1^j + B_2^i B_2^j + B_3^i B_3^j. \quad (12)$$

In this representation, \mathbf{B}_1 and \mathbf{B}_2 have radial and azimuthal components, while \mathbf{B}_3 is purely axial [23],

$$\mathbf{B}_{1,2} = \left(\frac{\eta_p}{2\tau} \right)^{1/2} \begin{bmatrix} -1 \\ \text{Wi} \pm (\text{Wi}^2 + 1)^{1/2} \\ 0 \end{bmatrix}, \quad (13)$$

$$\mathbf{B}_3 = \left(\frac{\eta_p}{\tau} \right)^{1/2} \begin{bmatrix} 0 \\ 0 \\ 1 \end{bmatrix}. \quad (14)$$

A general analysis of the instability requires expansion of the nonlinear Eqs. (8) and (10) in small deviations from the basic flow. Depending on what deviations are considered, different “magnetic fields” play dominant roles. If one assumes that the perturbations are axisymmetric ($k_\theta = 0$), and their wavevectors obey $k_z \gg k_r$, then the azimuthal and radial fields $\mathbf{B}_{1,2}$ are not relevant for the instability, and the dominant role is played by the axial field \mathbf{B}_3 , in direct analogy with the corresponding magnetorotational instability.

TABLE I. Summary of experiments. C is the polymer concentration. The relaxation time τ is estimated from numerical simulations of the Oldroyd- B model.

C (%)	$\dot{\gamma}_c$ (s^{-1})	η_p (Pa s)	λ_z (mm)	m	Re	Wi	τ (s)
0.5	7.3	0.19	30	0	14	4.4	0.57
0.375	6.5	0.11	29	± 1	21	2.8	0.44
0.25	5.6	0.056	21	± 1	36	1.9	0.34
0.19	Turb						

II. EXPERIMENT

In our experiment, a polymer fluid fills the gap between two coaxial cylinders rotating in the same direction with different angular velocities. The gap is narrow, and the cylinders are driven by the same motor with two different gears. The gears are chosen as to approximate the Keplerian velocity profile $\Omega(r) \propto r^{-3/2}$ in the gap. (In fact, any profile where the outer cylinder rotates slower than the inner one, but the specific angular momentum of the outer cylinder is larger than that of the inner one is suitable for the considered instability.)

The outer diameter of the inner cylinder is 14", the inner diameter of the outer cylinder is 15.5", and the height of the cylinders is 2'. The outer cylinder is transparent and the flow is visualized by adding a small amount of highly reflecting Kalliroscope particles. The angular velocity of rotation can reach 40 rad/s, which, for the Keplerian velocity profile translates into a shearing rate $\dot{\gamma} \equiv \partial v_\theta / \partial r - v_\theta / r \approx 60 \text{ s}^{-1}$.

For the polymer fluid, we chose an aqueous solution of high molecular weight Polyethylene Oxide ($M_W \approx 7\,000\,000 \text{ g/mole}$) obtained from DOW Chemical. The experiments were conducted at ambient temperature of 20 °C, although the temperature was not precisely controlled. First, we checked that in the studied range of angular velocities, the hydrodynamic flow without polymer additives was stable. We then performed a series of experiments with different concentrations of PolyOx. In each experiment, we gradually increased the rotation velocity to obtain the instability threshold. The results of four representative experiments are summarized in Table I.

No instability was observed for concentrations less than about 0.2% by weight, but rather at very high rotation rates turbulence set up at the ends of the cylinders where the Keplerian profile is broken, and propagated over the whole cylinder. At higher concentrations, however, the instability did appear. At the polymer concentration of 0.25%, the most unstable mode was a spiral $v(k) \propto \exp(ik_z z + im\theta)$ with azimuthal wave number $m = \pm 1$ and the axial wavelength $\lambda_z \approx 21 \text{ mm}$. Due to symmetry, the spirals winding up and down are equally probable. In different runs, the flow, therefore, spontaneously broke into regions of $m=1$ and $m=-1$, as, e.g., in Fig. 1, left panel. The threshold for this instability was about $\dot{\gamma}_c(0.25) \approx 5.6 \text{ s}^{-1}$.

As the concentration was increased further, the most unstable mode became axisymmetric. In particular, in the case of polymer concentration 0.5% by weight, the most unstable

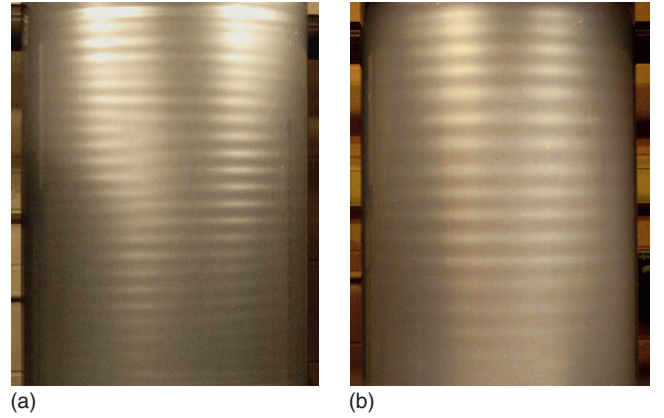


FIG. 1. (Color online) Elastorotational instability in viscoelastic Couette-Taylor flow. Left: most unstable mode is $m = \pm 1$ ($C = 0.25\%$). Right: most unstable mode is axisymmetric ($C = 0.5\%$).

mode had the wavelength $\lambda_z \approx 30 \text{ mm}$. The threshold for this instability was $\dot{\gamma}_c(0.5) \approx 7.3 \text{ s}^{-1}$. The result for 0.5% solution is shown in Fig. 1, right panel. In both cases, the instability was detectable by eye and the pattern was captured with a generic digital camera.

To argue that the observed instability is analogous to the magnetorotational instability, we performed another series of experiments. This time, the gears at the cylinders were chosen to set up either quasi-Keplerian $\Omega(r) \propto r^{-1.3}$ or “anti-Keplerian” $\Omega(r) \propto r^{1.3}$ profiles, so that the shearing rate in the anti-Keplerian profile has the inverted sign compared to that of the Keplerian profile. This is done to exclude the so-called elastic instability that can exist even for small Reynolds numbers ($\text{Re} = \dot{\gamma} d^2 / \eta_p$) as long as the Weissenberg number exceeds a certain threshold [27]. The elastic instability takes energy from the elastic energy of the flow, and should not essentially depend on the sign of $\partial\Omega/\partial r$, while for the MRI, the sign of $\partial\Omega/\partial r$ is crucial.

In the anti-Keplerian case, the only instability that could exist is purely elastic instability. For the considered concentrations of PolyOx, we observed the instability in the quasi-Keplerian case (analogous to the instability in the Keplerian case), however, we did not observe any instability in the anti-Keplerian case, even when we increased the shearing rates to three times as high as in the Keplerian counterpart. This indicates that in our Keplerian case, the observed instability is driven by inertia and takes its energy from the kinetic energy of the flow. We, therefore, propose that the observed “elastorotational” instability is analogous to the magnetorotational instability.

III. DISCUSSION

Certain support for our observations is provided by the Ogilvie-Proctor consideration outlined in previous sections. We should be cautioned, however, that this model is to some extent phenomenological. It is known that the polymer fluid viscosity η_p and relaxation time τ are not constants, but they strongly decrease as the shearing rate increases beyond $\dot{\gamma}\tau \approx 1$ (the effect of shear-thinning). Besides, a model with

single relaxation time is often not adequate, and one needs to introduce a series of relaxation times describing the relation between the shear rate and stress tensor. More essential, however, is the fact that in our case the polymer solution cannot be considered dilute for the used polymer concentrations. The application of the theory is, therefore, limited.

We, however, found that the theory is in reasonable agreement with the experiment if one substitutes the experimentally measured value for unknown viscosity η_p . Indeed, consider the case of the axisymmetric instability observed at polymer concentration 0.5%. We measured the shear viscosity of the flow η_p at the obtained critical shearing rate $\dot{\gamma}_c$ by measuring the viscosity in a Bohlin rheometer using a system of two coaxial cylinders—a scaled down copy of the experimental setup. The inner cylinder was stationary, and the outer cylinder rotated steadily, so that the shear rate in the gap matched the shear rate in the experiment. The measured viscosity was $\eta_p(0.5) \approx 190$ mPa·s. As for the relaxation time, it can be found for very low shearing rates using oscillation measurements, giving the value of order $\tau_0(0.5) \sim 1.4$ s. The relaxation time is, however, strongly shear-thinned at the experimental shear rate, so its precise value is difficult to evaluate.

We now substitute the experimental values of the critical shearing rate $\dot{\gamma}_c$, viscosity η_p , and the wave vector k_z , into the linearized Oldroyd- B equations. Such linearized equations are derived in the limit of small but nonvanishing d/R in [27]; they are bulky and not presented here. We solved these equations numerically. The solution confirms that the axisymmetric instability with the observed parameters indeed exists if the fluid relaxation time is $\tau \sim 0.6$ s. This is a reasonable number if shear-thinning is taken into account. With this relaxation time, we estimate that the instability occurs at $Wi = \dot{\gamma}\tau \sim 4.4$ and $Re = \dot{\gamma}d^2/\eta_p \sim 14$. Moreover, when we numerically switched to the anti-Keplerian profile by inverting the sign of the shearing rate $\dot{\gamma}$, the instability disappeared, which agrees with the experiment.

We note a useful fact that in the axisymmetric case ($m=0$), the instability threshold involves only axial field $B_3 = \sqrt{\eta_p/\tau}$. In the kinetic theory of dilute polymer solutions the ratio η_p/τ is constant and proportional only to polymer concentration (e.g., [28]; we thank Michael Graham for pointing this out). Therefore, the “imposed magnetic field” \mathbf{B}_3 is stable even when both polymer viscosity and relaxation time are shear-thinned by the flow. In the nonaxisymmetric case ($m \neq 0$), however, the instability also depends on the azimuthal field $\mathbf{B}_{1,2}$. In principle, it may be possible to design an experiment where such azimuthal field dominates, which would provide even closer analogy with real accretion disks.

Finally, we comment on previously studied instabilities in Couette-Taylor flows of polymer fluids, which we can broadly divide into inertioelastic and purely elastic, see a review in [29]. In particular, inertioelastic instabilities for a variety of velocity profiles were characterized in, e.g., [30,31], while the purely elastic instability was studied in [27,32]. It is crucial to note that in all previous studies of the inertioelastic instabilities, the chosen velocity profiles were such that they would become hydrodynamically unstable even without polymers if the Reynolds numbers were high enough. In contrast, in our case, the Keplerian-like velocity profiles are hydrodynamically stable at any Reynolds number (any rotation rate).

The purely elastic instability, on the other hand, can exist even if the Reynolds number is arbitrarily small as long as the Weissenberg number exceeds certain threshold. The purely elastic instability is, therefore, not essentially sensitive to fluid inertia effects and, in particular, to the sign of the velocity shear. In contrast, the inertia effects and the sign of the velocity shear are crucial in our case. This is demonstrated experimentally—the instability disappears when the sign of the velocity shear is inverted. These observations may suggest that the instability we observed is not analogous to the previously studied inertioelastic and purely elastic instabilities. This conclusion is consistent with the fact that the mechanism of magnetorotational instability outlined in the introduction (see also, [3–5]) is qualitatively different from the mechanisms of previously studied polymer fluid instabilities, e.g., [27,29–33].

In conclusion, based on our results, we propose that the analog of magnetorotational instability can be experimentally studied in viscoelastic flows of polymer fluids. In future work, we plan to present more detailed characterization of the observed instability. For a more quantitative analysis and for closer comparison with the theory, different polymer solutions should be used whose viscosities are not strongly shear-thinned, the so-called Boger fluids [34]. This work is in progress.

ACKNOWLEDGMENTS

We are grateful to Mark Anderson, Riccardo Bonazza, Cary Forest, Michael Graham, and Daniel Klingenberg for discussions and help with the experiment. This work was supported by the Wisconsin Alumni Research Foundation. The work of S.B. and V.P. was supported by the NSF Center for Magnetic Self-Organization in Laboratory and Astrophysical Plasmas at the University of Wisconsin—Madison. The work of S.B. was also supported by the Department of Energy Grant No. DE-FG02-07ER54932.

-
- [1] D. Lynden-Bell, *Nature (London)* **223**, 690 (1969).
 [2] N. I. Shakura and R. A. Sunyaev, *Astron. Astrophys.* **24**, 337 (1973).
 [3] E. P. Velikhov, *Sov. Phys. JETP* **9**, 995 (1959).
 [4] S. Chandrasekhar, *Proc. Natl. Acad. Sci. U.S.A.* **46**, 253

- (1960).
 [5] S. Balbus and J. F. Hawley, *Astrophys. J.* **376**, 214 (1991).
 [6] J. Goodman and H. Ji, *J. Fluid Mech.* **462**, 365 (2002).
 [7] R. Hollerbach and G. Rüdiger, *Phys. Rev. Lett.* **95**, 124501 (2005).

- [8] D. Hughes and S. Tobias, Proc. R. Soc. London, Ser. A **457**, 1365 (2001).
- [9] S. Balbus and J. F. Hawley, Rev. Mod. Phys. **70**, 1 (1998).
- [10] J. F. Hawley, Astrophys. J. **528**, 462 (2000).
- [11] J. F. Hawley, Astrophys. J. **554**, 534 (2001).
- [12] J. F. Hawley, C. F. Gammie, and S. A. Balbus, Astrophys. J. **440**, 742 (1995).
- [13] K. A. Miller and J. M. Stone, Astrophys. J. **534**, 398 (2000).
- [14] A. Kageyama, H. Ji, J. Goodman, F. Chen, and E. Shoshan, J. Phys. Soc. Jpn. **73**, 2424 (2004).
- [15] K. Noguchi, V. I. Pariev, S. A. Colgate, H. F. Beckley, and J. Nordhaus, Astrophys. J. **575**, 1151 (2002).
- [16] E. P. Velikhov, A. A. Ivanov, V. P. Lakhin, and K. S. Serebrennikov, Phys. Lett. A **356**, 357 (2006).
- [17] G. Rüdiger, M. Schultz, and D. Shalybkov, Phys. Rev. E **67**, 046312 (2003).
- [18] A. P. Willis and C. F. Barenghi, Astron. Astrophys. **393**, 339 (2002).
- [19] D. Lathrop, The 47th Annual APS Meeting of the Division of Plasma Physics, 2005, paper FZ1.006 (unpublished).
- [20] D. R. Sisan, N. Mujica, W. A. Tillotson, Y. M. Huang, W. Dorland, A. B. Hassam, T. M. Antonsen, and D. P. Lathrop, Phys. Rev. Lett. **93**, 114502 (2004).
- [21] F. Stefani, T. Gundrum, G. Gerbeth, G. Rüdiger, M. Schultz, J. Szklarski, and R. Hollerbach, Phys. Rev. Lett. **97**, 184502 (2006).
- [22] W. Liu, J. Goodman, I. Herron, and H. Ji, Phys. Rev. E **74**, 056302 (2006).
- [23] G. I. Ogilvie and M. R. E. Proctor, J. Fluid Mech. **476**, 389 (2003).
- [24] G. I. Ogilvie and A. T. Potter, Phys. Rev. Lett. **100**, 074503 (2008).
- [25] R. B. Bird, R. C. Armstrong, and O. Hassager, *Dynamics of Polymeric Liquids*, 2nd ed. (Wiley, New York, 1987), Vol. 1.
- [26] J. G. Oldroyd, Proc. R. Soc. London, Ser. A **200**, 523 (1950).
- [27] R. G. Larson, E. S. G. Shaqfeh, and S. J. Muller, J. Fluid Mech. **218**, 573 (1990).
- [28] M. Doi and S. F. Edwards, *The Theory of Polymer Dynamics* (Oxford University Press, New York, 1986).
- [29] A. Groisman and V. Steinberg, New J. Phys. **6**, 29 (2004).
- [30] B. M. Baumert and S. J. Muller, J. Non-Newtonian Fluid Mech. **83**, 33 (1999).
- [31] O. Crumeyrolle, I. Mutabazi, and M. Grisel, Phys. Fluids **14**, 1681 (2002).
- [32] Y. K. Joo and E. S. G. Shaqfeh, J. Fluid Mech. **262**, 27 (1994).
- [33] P. Pakdel and G. H. McKinley, Phys. Rev. Lett. **77**, 2459 (1996).
- [34] D. V. Boger, J. Non-Newtonian Fluid Mech. **3**, 87 (1977).